

Platinum Complexes with a Phosphino-Oxime/Oximate Ligand

Javier Francos,^[a] Javier Borge,^[b] Salvador Conejero,^[c] and Victorio Cadierno^{*,[a]}

Abstract: The platinum(II) complex [PtCl₂(COD)] (**2**; COD = 1,5-cyclooctadiene) reacted with **1** and 2 equivalents of 2-(diphenylphosphino)benzaldehyde oxime (**1**) to generate [PtCl₂{κ²-(*P,N*)-2-Ph₂PC₆H₄CH=NOH}] (**3**) and [Pt{κ²-(*P,N*)-2-Ph₂PC₆H₄CH=NOH}₂][Cl]₂ (**4**), respectively. Deprotonation of the oxime hydroxyl group of **3** with Na₂CO₃ led to the selective formation of the dinuclear species (μ-O)-[PtCl{κ²-(*P,N*)-2-Ph₂PC₆H₄CH=NO}]₂ (**5**), while the related methylated derivative (μ-O)-[PtMe{κ²-(*P,N*)-2-Ph₂PC₆H₄CH=NO}]₂ (**7**) could be obtained from the direct reaction of [PtMe₂(COD)] (**6**) with the phosphino-oxime ligand **1**. In the case of **4**, its treatment with Na₂CO₃ yielded complex [Pt{κ²-(*P,N*)-2-Ph₂PC₆H₄CH=NO₂H}][Cl] (**8**), as a result of the deprotonation of only one of the OH groups of **4**. On the other hand, contrary to what it was observed with **6**, no deprotonation of the oxime occurred in the reaction of [PtMe₃]₄ (**9**) with **1**, from which the mononuclear Pt(IV) derivative *fac*-[PtMe₃{κ²-(*P,N*)-2-Ph₂PC₆H₄CH=NOH}] (**10**) was isolated. The solid-state structures of compounds **3**, **4**, **7** and **10** were determined by X-ray crystallography. In addition, the potential of all the synthesized complexes as catalysts for the dehydrogenative coupling of hydrosilanes with alcohols is also briefly discussed.

Introduction

Hybrid bidentate ligands are ubiquitous in coordination chemistry and homogeneous catalysis.^[1] Since the electronic properties of each donor atom in this type of ligands are different, once coordinated to a metal center, they have the potential to create distinct binding sites in the *trans* positions, thus influencing the reactivity patterns of the complexes and the selectivity for particular products in the catalytic reactions. Importantly, hybrid ligands usually present hemilability, a particularly advantageous property in catalysis since the reversible dissociation of one of the two donor atoms temporarily creates an open coordination site for

substrate binding, the facile re-association of the ligand imparting for its side stability to the catalyst in its resting state.^[2]

Given that phosphorus and nitrogen donors are prevalent in coordination chemistry, bidentate mixed *P,N*-donor ligands are by far the most common hybrid ligands found in the literature.^[1,2] Prototypical examples are the phosphino-imines 2-Ph₂PC₆H₄CH=NR (**A** in Figure 1), easily accessible by condensation of 2-(diphenylphosphino)benzaldehyde with both aromatic and aliphatic primary amines. A large number of these ligands, including chiral examples, are currently known, featuring a rich coordination chemistry and application in different research areas including catalysis.^[3]

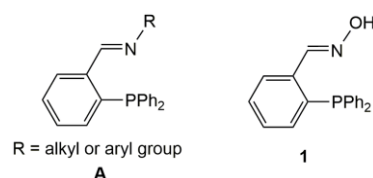


Figure 1. Structure of the phosphino-imines **A** and the phosphino-oxime ligand **1**.

In marked contrast, little is known about the chemistry of the related phosphino-oxime derivative **1** (Figure 1),^[4] a rather surprising fact given the commercial availability of this compound^[5] and the presence in its structure of a non-innocent hydroxyl functionality.^[6] Thus, the deprotonation of this OH group would allow the generation of the corresponding oximate anion, thereby conferring to **1** a greater coordination versatility compared to compounds **A**.^[7] On the other hand, the cooperative effects that the inclusion of hydroxyl substituents in the structure of ligands exert in catalysis are now widely recognized and exploited for the design of new bifunctional catalysts, so compound **1** would also be useful in this area.^[8]

All these facts prompted us to initiate studies aimed at exploiting the potential of ligand **1** in coordination chemistry and homogeneous catalysis. As a result, we recently reported the preparation of the palladium(II) complexes **B** and **C** (Figure 2). Interestingly, these compounds proved to be efficient catalysts for the rearrangement and dehydration of aldoximes to generate, respectively, primary amides and nitriles, featuring for both processes catalytic activities superior to those previously described with other Pd(II)-based catalysts.^[9] Moreover, we also synthesized the ruthenium derivatives **D** and **E** (Figure 2), which proved to be useful catalysts for the synthesis of secondary aryl-carbinols by α -alkylation/reduction of acetophenone derivatives with primary alcohols.^[10] Besides, the only additional works involving **1** that can be found in the literature are: (i) its use as auxiliary ligand in copper-catalyzed arylation reactions^[11] and (ii) in palladium-catalyzed Suzuki-Miyaura cross-coupling processes,^[12] although in none of these studies the corresponding metal complexes were isolated.

[a] Laboratorio de Compuestos Organometálicos y Catálisis (Unidad Asociada al CSIC), Centro de Innovación en Química Avanzada (ORFEO-CINQA), Departamento de Química Orgánica e Inorgánica, Instituto Universitario de Química Organometálica "Enrique Moles", Universidad de Oviedo, Julián Clavería 8, E-33006 Oviedo, Spain
E-mail: francosjavier@uniovi.es (J.F.), vcm@uniovi.es (V.C.)
Homepage: <http://www.unioviado.es/comorca>

[b] Departamento de Química Física y Analítica, Centro de Innovación en Química Avanzada (ORFEO-CINQA), Facultad de Química, Universidad de Oviedo, Julián Clavería 8, E-33006 Oviedo, Spain

[c] Instituto de Investigaciones Químicas (IIQ), Departamento de Química Inorgánica, Centro de Innovación en Química Avanzada (ORFEO-CINQA), CSIC and Universidad de Sevilla, Avda. Américo Vespucio 49, E-41092 Sevilla, Spain
E-mail: sconejero@iiq.csic.es
Homepage: <http://www.sconejero.wixsite.com/amorysalva-chemistry>

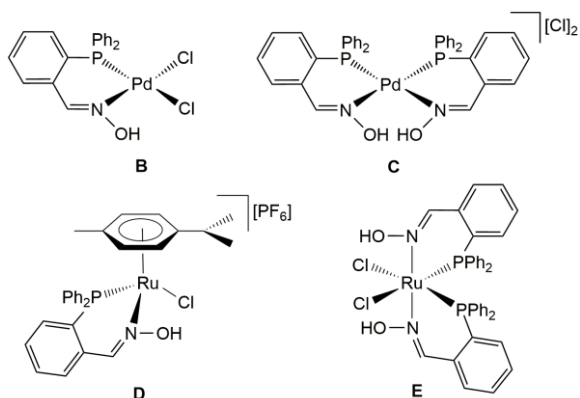
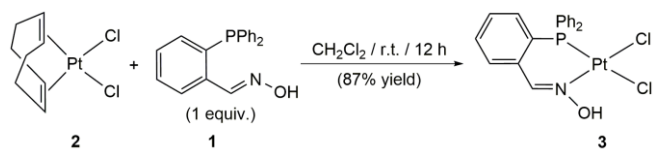


Figure 2. Structure of the phosphino-oxime Pd(II) and Ru(II) complexes **B-E**.

As a continuation of our studies on the chemistry of 2-(diphenylphosphino)benzaldehyde oxime **1**, herein we report on the reactivity of this ligand towards the Pt(II) and Pt(IV) precursors [PtCl₂(COD)] (COD = 1,5-cyclooctadiene), [PtMe₂(COD)] and [PtMe₃]₄, along with an evaluation of the resulting complexes as potential catalysts for the cross dehydrogenative coupling of hydrosilanes with alcohols. Interestingly, as a result of this work, the first examples of metal complexes containing the oximate anion derived from **1** have been synthesized.

Results and Discussion

In our previous study with palladium, the cyclooctadiene-Pd(II) complex [PdCl₂(COD)] was found to be the most appropriate starting material for the preparation of compounds **B** and **C** (Figure 2).¹⁹ Based on this, we decided to start our investigations exploring the reactivity of the phosphino-oxime ligand **1** towards the analogous Pt(II) precursor [PtCl₂(COD)] (**2**). Thus, we found that the treatment of a dichloromethane solution of this complex with a stoichiometric amount of **1**, at room temperature overnight, leads to the selective formation of the mononuclear derivative [PtCl₂{κ²-(*P,N*)-2-Ph₂PC₆H₄CH=NOH}] (**3**), via the expected exchange of the labile 1,5-cyclooctadiene ligand (Scheme 1).



Scheme 1. Synthesis of the Pt(II) complex [PtCl₂{κ²-(*P,N*)-2-Ph₂PC₆H₄CH=NOH}] (**3**).

The characterization of this compound, isolated as an air-stable yellow solid in 87% yield, was achieved by means of standard spectroscopic techniques (IR and multinuclear NMR), high-resolution mass spectrometry and elemental analyses, all data being fully consistent with the proposed formulation (see the Experimental Section for details). In particular, the coordination of

1 to platinum was evidenced in the ³¹P{¹H} NMR spectrum of **3** by the appearance of a singlet resonance at δ_P 1.1 ppm, downfield shifted with respect to that of the free ligand **1** (δ_P -14.5 ppm), and featuring the expected ¹⁹⁵Pt satellites (*J*_{Pt,P} = 3735.0 Hz). In the ¹H and ¹³C{¹H} NMR spectra of **3**, the most informative signals were those associated to the aldoxime CH=NOH protons and carbon, which resonate at δ_H 8.53 (s, *J*_{Pt,H} = 77.6 Hz, CH=N) and 11.99 (s, OH) ppm, and δ_C 147.2 (d, *J*_{P,C} = 6.1 Hz, *J*_{Pt,H} = 59.7 Hz) ppm, respectively.

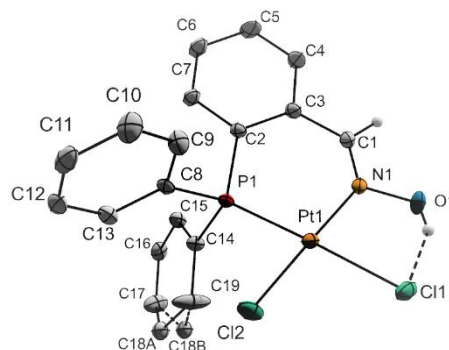
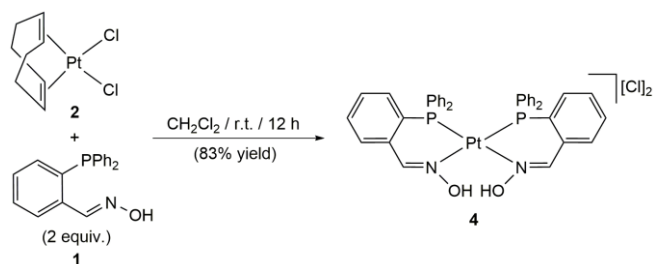


Figure 3. ORTEP-type view of the structure of complex **3** showing the crystallographic labelling scheme. Aromatic hydrogen atoms have been omitted for clarity. Thermal ellipsoids are drawn at 30% probability level. Selected bond lengths [Å] and angles [°]: Pt-Cl(1) 2.3818(9); Pt-Cl(2) 2.284(1); Pt-P(1) 2.2136(9); Pt-N(1) 2.008(3); C(1)-N(1) 1.279(5); N(1)-O(1) 1.408(4); Cl(1)-Pt-Cl(2) 88.41(4); Cl(1)-Pt-P(1) 177.04(4); Cl(1)-Pt-N(1) 90.26(2); Cl(2)-Pt-P(1) 88.70(3); Cl(2)-Pt-N(1) 178.56(9); P(1)-Pt-N(1) 92.63(9); C(3)-C(1)-N(1) 127.5(4); C(1)-N(1)-O(1) 110.2(3); C(1)-N(1)-Pt 133.2(3); Pt-N(1)-O(1) 116.6(3).

Moreover, the structure of this complex was corroborated through a single-crystal X-ray diffraction study. X-ray quality crystals were obtained by slow diffusion of hexanes into a saturated solution of **3** in a dichloromethane/methanol mixture (3:1 v/v). An ORTEP view of the molecule, along with selected structural parameters, is shown in Figure 3. As expected, a square planar geometry around the metal is observed, with a maximum deviation from the mean PtCl₂PN plane of 0.0091(7) Å for the platinum atom. The two chloride ligands are mutually *cis* disposed, with the larger Pt-Cl(1) vs Pt-Cl(2) bond length found (2.3818(9) vs 2.284(1) Å) being consistent with the stronger *trans* influence of phosphorus compared to nitrogen. These distances, along with the Pt-P(1) (2.2136(9) Å) and Pt-N(1) (2.008(3) Å) ones, are comparable to those described in the literature for related Pt(II) complexes containing the more classical phosphino-imines **A** (Fig. 1).^[3i,3j,13] Similarly, the C(1)-N(1) and N(1)-O(1) bond lengths (1.279(5) and 1.408(4) Å) show typical values for an aldoxime unit coordinated to a platinum(II) center.^[14] On the other hand, the close proximity of the hydroxyl-oxime function to one of the chloride ligands enabled the establishment of an intramolecular hydrogen bond between both groups.^[15] The distances and angles of the O(1)-H(1o)···Cl(1) contact (O(1)-H(1o) = 0.95(8) Å, H(1o)-Cl(1) = 2.05(8) Å, O(1o)-Cl(1) = 2.930(4) Å and O(1)-H(1o)-Cl(1) = 153.0(6)°) indicate, according to Jeffrey's scale,^[16] that the intensity of this H-bond is only moderate (mostly electrostatic).



Scheme 2. Synthesis of the Pt(II) complex $[\text{Pt}\{\kappa^2\text{-}(P,N)\text{-}2\text{-Ph}_2\text{PC}_6\text{H}_4\text{CH=NOH}\}_2][\text{Cl}]_2$ (**4**).

As previously observed with $[\text{PdCl}_2(\text{COD})]$,^[9] the treatment of $[\text{PtCl}_2(\text{COD})]$ (**2**) with two equivalents of **1** also allows the coordination of the molecules of the phosphine-oxime ligand to platinum. Thus, the reaction, performed in dichloromethane at room temperature, allowed the isolation of the dicationic species $[\text{Pt}\{\kappa^2\text{-}(P,N)\text{-}2\text{-Ph}_2\text{PC}_6\text{H}_4\text{CH=NOH}\}_2][\text{Cl}]_2$ (**4**) in 83% yield (Scheme 2). The structure of **4** was unequivocally confirmed by X-ray diffraction, after crystallization of the complex using the same procedure described above for the neutral derivative **3**. Crystals containing methanol molecules of solvation were in this case obtained, with two crystallographically independent molecules of the complex and four MeOH molecules being present in the asymmetric unit. An ORTEP view of the metal dication is shown in Figure 4, along with selected bond distances and angles (given the similarity between their respective structural parameters, we only show and give the data of one of the two independent molecules found in the asymmetric unit). The stereochemistry found, with the two PPh_2 and oxime groups mutually *cis* disposed, is consistent with that previously observed in the crystal structure of the analogous Pd(II) derivative $[\text{Pd}\{\kappa^2\text{-}(P,N)\text{-}2\text{-Ph}_2\text{PC}_6\text{H}_4\text{CH=NOH}\}_2][\text{Cl}]_2$ (**C** in Figure 2).^[9,17] The steric repulsions between the PPh_2 groups resulting from this arrangement lead to a greater deviation from the ideal square planar geometry compared to the case of the neutral complex $[\text{PtCl}_2\{\kappa^2\text{-}(P,N)\text{-}2\text{-Ph}_2\text{PC}_6\text{H}_4\text{CH=NOH}\}]$ (**3**). In line with this, a maximum deviation from the mean PtP_2N_2 plane of 0.2758(2) Å was found for the N(1A) atom. Nonetheless, the bond distances and angles within the two phosphino-oxime skeletons were almost identical to those observed for **3**, reflecting that, once coordinated, the structure of the ligand is non-sensitive to the platinum environment.^[18]

Concerning the characterization in solution of complex **4**, its $^{31}\text{P}\{^1\text{H}\}$ NMR spectrum in CD_2Cl_2 showed the presence of a singlet resonance at $\delta_{\text{P}} 6.1$ ppm ($J_{\text{Pt,P}} = 3620.6$ Hz), while broad unresolved signals were found in the ^1H and $^{13}\text{C}\{^1\text{H}\}$ NMR spectra (see the Experimental Section). A similar fact had been previously observed by us when characterizing the analogous Pd(II) derivative **C** (Figure 2), as a result of the fluxional behaviour of this complex in solution derived from the hemilabile character of the phosphino-oxime ligand **1**.^[9] The low molar conductivity showed by **4** in dimethylsulfoxide ($\Lambda = 31 \Omega^{-1}\cdot\text{cm}^2\cdot\text{mol}^{-1}$), falling within the typical range for 1:1 electrolytes,^[19] seems to suggest an analogous behaviour for this Pt(II) complex (see Scheme 3).

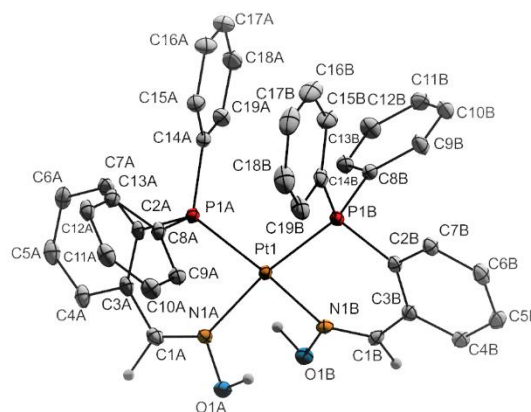
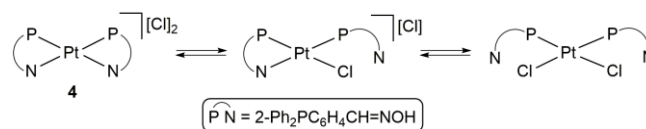
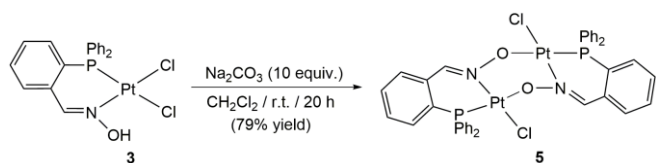


Figure 4. ORTEP-type view of the structure of complex **4** showing the crystallographic labelling scheme. Aromatic hydrogen atoms, chloride anions and methanol solvent molecules have been omitted for clarity. Thermal ellipsoids are drawn at 30% probability level. Selected bond lengths [Å] and angles [°]: Pt-P(1A) 2.2529(8); Pt-P(1B) 2.2351(9); Pt-N(1A) 2.088(3); Pt-N(1B) 2.091(3); C(1A)-N(1A) 1.271(5); C(1B)-N(1B) 1.278(5); N(1A)-O(1A) 1.402(4); N(1B)-O(1B) 1.394(4); P(1A)-Pt-N(1A) 88.57(8); P(1A)-Pt-N(1B) 168.13(9); P(1A)-Pt-P(1B) 99.52(3); N(1A)-Pt-N(1B) 89.5(1); N(1A)-Pt-P(1B) 163.57(9); N(1B)-Pt-P(1B) 88.22(9); C(3A)-C(1A)-N(1A) 123.8(3); C(3B)-C(1B)-N(1B) 126.3(3); C(1A)-N(1A)-O(1A) 113.3(3); C(1B)-N(1B)-O(1B) 113.5(3); Pt-N(1A)-O(1A) 114.4(2); Pt-N(1B)-O(1B) 113.7(2); Pt-N(1A)-C(1A)-132.3(3); Pt-N(1B)-C(1B)-132.8(3).



Scheme 3. Proposed behaviour in solution for $[\text{Pt}\{\kappa^2\text{-}(P,N)\text{-}2\text{-Ph}_2\text{PC}_6\text{H}_4\text{CH=NOH}\}_2][\text{Cl}]_2$ (**4**).

On the other hand, it is well-known that, upon coordination to a metal center, the acidity of the hydroxyl group of oximes is considerably enhanced,^[7] so we considered of interest to carry out a study of the behaviour of complexes **3** and **4** in basic medium and thus to evaluating the possibility of forming new oximato-Pt(II) derivatives.^[20] In this regard, we found that the treatment of a CH_2Cl_2 solution of $[\text{PtCl}_2\{\kappa^2\text{-}(P,N)\text{-}2\text{-Ph}_2\text{PC}_6\text{H}_4\text{CH=NOH}\}]$ (**3**) with an excess of Na_2CO_3 results in the clean formation of a new species **5** featuring a singlet resonance in its $^{31}\text{P}\{^1\text{H}\}$ NMR spectrum at $\delta_{\text{P}} 0.7$ ppm ($J_{\text{Pt,P}} = 3859.1$ Hz), a chemical shift very close to that of **3** ($\delta_{\text{P}} 1.1$ ppm; $J_{\text{Pt,P}} = 3735.0$ Hz). The IR and ^1H NMR spectra recorded for this compound confirmed the deprotonation of the oxime OH group, lacking the characteristic $\nu(\text{OH})$ stretching vibration and the downfield proton signal of this functionality, respectively. This fact, together with the observation of all the expected signals for the rest of the *P,N*-donor ligand skeleton by ^1H and $^{13}\text{C}\{^1\text{H}\}$ NMR spectroscopy (see the Experimental Section), led us to propose for **5** the dinuclear structure depicted in Scheme 4. The data obtained by electrospray ionization mass spectrometry (ESI-HRMS) corroborated this proposal, the spectrum displaying the corresponding $[\text{M} - \text{Cl}]^+$ ion peak at $m/z 1033.0766$.



Scheme 4. Synthesis of the dinuclear platinum(II) complex (μ -O)-[PtCl(κ^2 -(*P,N*)-2-Ph₂PC₆H₄CH=NO)]₂ (**5**).

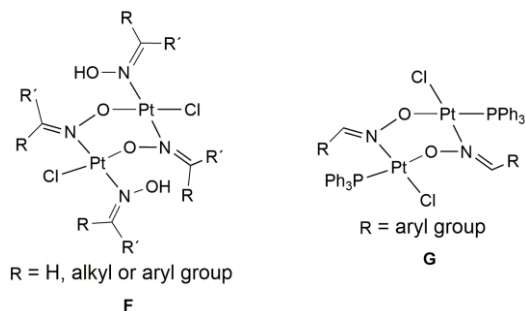
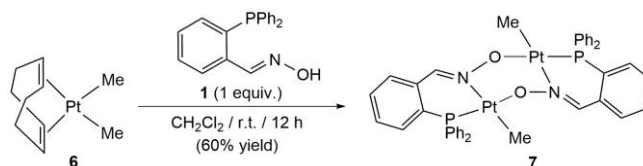


Figure 5. Structure of oximate-bridged dinuclear Pt(II) species **F** and **G**.

At this point we would like to remark that the only precedents of oximate-bridged dinuclear Pt(II) complexes found in the literature are compounds **F**^[14b] and **G**^[14d] (Figure 5), generated by deprotonation of the corresponding mononuclear species [PtCl₂{ κ^1 -(*N*)-N(OH)=CRR'}₂] and [PtCl₂{ κ^1 -(*N*)-N(OH)=CHR}(PPh₃)], respectively. Moreover, in the case of compounds **F** their structures could be unambiguously established by X-ray diffraction. Unfortunately, in our case, all attempts to obtain crystals of **5** suitable for X-ray diffraction studies failed. Nonetheless, we succeeded in the crystallization of the related complex (μ -O)-[PtMe(κ^2 -(*P,N*)-2-Ph₂PC₆H₄CH=NO)]₂ (**7**). As shown in Scheme 5, this dinuclear compound was obtained by reacting the dimethyl-Pt(II) precursor [PtMe₂(COD)] (**6**) with the phosphine-oxime ligand **1**, as a result of the direct deprotonation of the oxime unit by one of the methyl groups coordinated to platinum, with concomitant release of methane. Complex **7** was isolated as an air-stable yellow solid in 60% yield, and we found that it is selectively formed irrespective of the stoichiometry employed in the reaction (**6**:**1** ratio of 1:1 or 1:2). As in the case of **3** and **4**, X-ray quality crystals of **7** were obtained by slow diffusion of hexanes into a saturated solution of the complex in a CH₂Cl₂/MeOH mixture (3:1 v/v). An ORTEP view of the molecule, where half is generated by symmetry due to the presence of crystallographic C₂ axis that passes through the center of the central 6-membered ring of the pentacyclic structure, is shown in Figure 6 (selected bond distances and angles are listed in the caption). This central metallacycle adopts a boat conformation, thus locating the two platinum atoms in a close proximity.^[21] The Pt...Pt distance observed of 3.3233(6) Å, shorter than the sum of the van der Waals radius for two Pt atoms (3.44 Å), indicates that, similar to the case of **F**,^[14b] a weak non-bonding metal-metal attractive interaction is present in the structure. The Pt-N(1) and Pt-O(1) bond lengths (2.090(6) and 2.105(5) Å, respectively), are also comparable to those found for compounds

F, and the Pt-C(20) one (2.051(8) Å) is typical for a Pt(II)-Me bond.^[22]



Scheme 5. Synthesis of the dinuclear platinum(II) complex (μ -O)-[PtMe(κ^2 -(*P,N*)-2-Ph₂PC₆H₄CH=NO)]₂ (**7**).

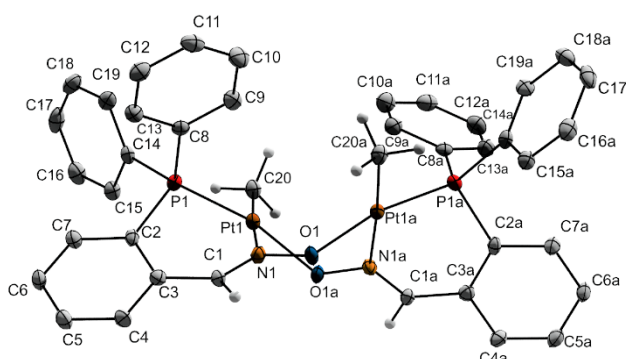
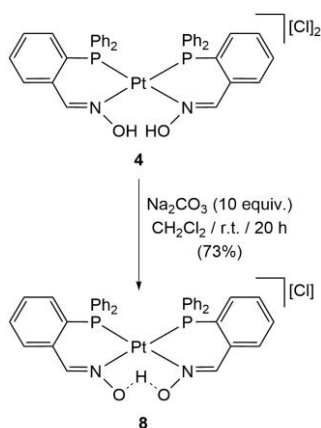


Figure 6. ORTEP-type view of the structure of complex **7** showing the crystallographic labelling scheme. Atoms labelled with an "a" are generated by a crystallographic 2-fold symmetry axis. Aromatic hydrogen atoms and methanol solvent molecules have been omitted for clarity. Thermal ellipsoids are drawn at 30% probability level. Selected bond lengths [Å] and angles [°]: Pt-P(1) 2.176(2); Pt-N(1) 2.090(6); Pt-O(1a) 2.105(5); Pt-C(20) 2.051(8); C(1)-N(1) 1.29(1); N(1)-O(1) 1.372(8); P(1)-Pt-N(1) 86.7(2); P(1)-Pt-O(1a) 167.7(2); P(1)-Pt-C(20) 96.3(2); N(1)-Pt-O(1a) 90.2(2); N(1)-Pt-C(20) 176.3(3); C(20)-Pt-O(1a) 87.2(3); C(3)-C(1)-N(1) 125.2(7); C(1)-N(1)-O(1) 114.5(6); Pt-N(1)-O(1) 117.0(4); Pt-N(1)-C(1) 128.4(5); N(1)-O(1)-Pt(a) 118.0(4).

Characterization of **7** by means of elemental analysis, IR and multinuclear NMR spectroscopy, and HRMS was also performed, the data obtained being in fully accord with the structure found in the solid state (details are given in the Experimental Section). In particular, the most characteristic spectroscopic features of this compound are: (i) (³¹P{¹H} NMR) a singlet resonance at δ_P 11.6 ppm ($J_{Pt,P} = 4412.3$ Hz), (ii) (¹H and ¹³C{¹H} NMR) the presence of characteristic resonances for the oximate and methyl groups at δ_H 8.25 (s, $J_{Pt,H} = 31.8$ Hz, CH=N) and 0.02 (d, $J_{P,H} = 1.8$ Hz and $J_{Pt,H} = 64.8$ Hz, Me) ppm, and δ_C 143.6 (virtual t, $N = 9.8$ Hz, CH=N) and -10.2 (d, $J_{P,C} = 5.8$ Hz, Me) ppm.

Concerning the behaviour of the dicationic complex [Pt(κ^2 -(*P,N*)-2-Ph₂PC₆H₄CH=NOH)₂][Cl]₂ (**4**), we found that it also reacts with sodium carbonate under mild conditions (r.t.) to generate in this case a new mononuclear species formulated as [Pt(κ^2 -(*P,N*)-2-Ph₂PC₆H₄CH=NO)₂H][Cl] (**8**) (Scheme 6). This compound results from the deprotonation of only one of the two phosphino-oxime ligands present in **4**,^[23] with the remaining OH group establishing an intramolecular H-bond interaction with the oxygen atom of the oximate anion formed. Although the structure of this compound could not be confirmed by X-ray diffraction, and the

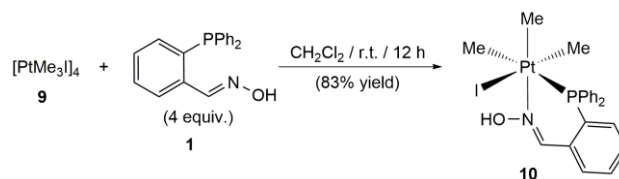
presence of the O-H-O proton was not observed in its ^1H NMR spectrum, the data obtained by HRMS (presence of the expected molecular ion peak $[\text{M}]^+$ at m/z 804.1483), IR spectroscopy (presence of a typical strong O-H-O absorption at 1741 cm^{-1})^[24] and conductance measurements ($\Lambda = 26.2\ \Omega^{-1}\cdot\text{cm}^2\cdot\text{mol}^{-1}$ in DMSO solution)^[19] were in agreement with our proposal. In addition, the NMR spectra recorded were fully consistent with the presence of a symmetry plane in the molecule as evidenced by the appearance of (i) a singlet resonance in the $^{31}\text{P}\{^1\text{H}\}$ NMR spectrum ($\delta_{\text{P}} 5.6\text{ ppm}$; $J_{\text{P},\text{P}} = 3273.6\text{ Hz}$), and (ii) a single set of signals for the phosphine ligands in the ^1H and $^{13}\text{C}\{^1\text{H}\}$ NMR spectra (in the latter, a second order pattern was observed for some of the aromatic carbons; see details in the Experimental Section).



Scheme 6. Synthesis of the mononuclear platinum(II) complex $[\text{Pt}\{\kappa^2\text{-}(P,N)\text{-}2\text{-Ph}_2\text{PC}_6\text{H}_4\text{CH=NO}_2\text{H}\}][\text{Cl}]$ (**8**).

On the other hand, the easy deprotonation of the oxime unit observed in the reaction of **1** with $[\text{PtMe}_2(\text{COD})]$ (**6**) (Scheme 5) encouraged us to study the behaviour of **1** towards the tetranuclear heterocubane Pt(IV) complex $[\text{PtMe}_3]_4$ (**9**).^[25] Thus, we found that, contrary to what happened with **6**, the treatment of a dichloromethane solution of tetramer **9** with a 4-fold excess of **1** at r.t. does not lead to the deprotonation of oxime unit of **1**, the reaction yielding the mononuclear derivative *fac*- $[\text{PtMe}_3\{\kappa^2\text{-}(P,N)\text{-}2\text{-Ph}_2\text{PC}_6\text{H}_4\text{CH=NOH}\}]$ (**10**) which could be isolated in 83% yield (Scheme 7).^[26] Characterization of this complex was straightforward following its analytical and spectroscopic data (see details in the Experimental Section), with key features being as follows: (i) ($^{31}\text{P}\{^1\text{H}\}$ NMR) a singlet resonance at $\delta_{\text{P}} -0.2\text{ ppm}$,^[27] (ii) (^1H NMR) characteristic resonances for the hydroxyl and iminic protons of the aldoxime fragment at $\delta_{\text{H}} 13.05$ (broad s) and 8.29 (s, $J_{\text{P},\text{H}} = 19.2\text{ Hz}$), respectively, as well as three high-field singlets for the Pt-coordinated methyl groups ($\delta_{\text{H}} 1.06$, 1.33 and 1.52 ppm , with $J_{\text{P},\text{H}}$ coupling constants ranging from 59.6 to 80.4 Hz), and (iii) ($^{13}\text{C}\{^1\text{H}\}$ NMR) the expected resonances for the C=N (a singlet at $\delta_{\text{C}} 151.5\text{ ppm}$) and Me carbons (three singlets at $\delta_{\text{C}} 6.6$, 7.8 and 8.9 ppm , with $J_{\text{P},\text{C}}$ coupling constants ranging from 535.7 to 643.7 Hz). The chemical inequivalence of the methyl ligands observed by NMR suggests their *facial* arrangement, a fact that was subsequently confirmed through a single-crystal X-ray diffraction

study. A view of the molecular structure is shown in Figure 7. Selected bond lengths and angles are given in the figure caption.



Scheme 7. Synthesis of the platinum(IV) complex *fac*- $[\text{PtMe}_3\{\kappa^2\text{-}(P,N)\text{-}2\text{-Ph}_2\text{PC}_6\text{H}_4\text{CH=NOH}\}]$ (**10**).

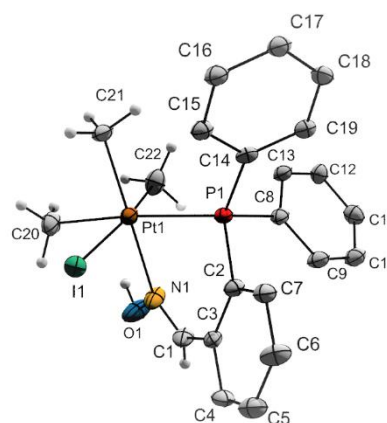
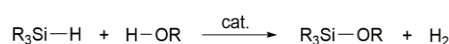


Figure 7. ORTEP-type view of the structure of complex **10** showing the crystallographic labelling scheme. Aromatic hydrogen atoms have been omitted for clarity. Thermal ellipsoids are drawn at 30% probability level. Selected bond lengths [Å] and angles [°]: Pt-P(1) 2.381(1); Pt-N(1) 2.176(6); Pt-I(1) 2.814(1); Pt-C(20) 2.104(7); Pt-C(21) 2.076(6); Pt-C(22) 2.084(9); C(1)-N(1) 1.26(1); N(1)-O(1) 1.419(9); P(1)-Pt-N(1) 82.5(1); P(1)-Pt-I(1) 91.59(4); P(1)-Pt-C(20) 175.3(2); P(1)-Pt-C(21) 99.6(2); P(1)-Pt-C(22) 94.0(2); N(1)-Pt-I(1) 90.3(2); N(1)-Pt-C(20) 93.2(3); N(1)-Pt-C(21) 176.6(3); N(1)-Pt-C(22) 92.1(4); I(1)-Pt-C(20) 86.6(3); I(1)-Pt-C(21) 92.4(3); I(1)-Pt-C(22) 174.2(2); C(20)-Pt-C(21) 84.8(3); C(20)-Pt-C(22) 88.0(4); C(21)-Pt-C(22) 85.0(4); C(3)-C(1)-N(1) 127.1(6); C(1)-N(1)-O(1) 112.9(6); Pt-N(1)-C(1) 130.8(6); Pt-N(1)-O(1) 116.3(5).

The platinum atom is in a slightly distorted octahedral environment surrounded by the three methyls, one iodide and the $\kappa^2\text{-}(P,N)$ -coordinated phosphino-oxime ligand **1**. The Pt-P(1) and Pt-N(1) bond lengths observed (2.381(1) and 2.176(6) Å, respectively) were both longer to those found in the structures of compounds **3**, **4** and **7**, likely due to the strong *trans* influence of the methyl ligands. Following a similar reasoning, the higher *trans* effect of P vs I and N would also explain the longer Pt-C(20) distance (2.104(7) Å) compared to the Pt-C(21) and Pt-C(22) ones (2.076(6) and 2.084(9) Å, respectively), with the three distances falling within the expected range for Pt(IV)-Me bonds (which usually lie between 2.01 and 2.15 Å).^[22] The Pt-I(1) bond length found (2.814(1) Å) is also typical for trimethylplatinum(IV) iodide complexes.^[28] Concerning the oxime unit, the change in the oxidation state of the metal has a negligible effect on its bonding, as reflected by the fact that the C(1)-N(1) and N(1)-O(1) distances in **10** were very similar (ca. 0.01 Å) to those observed for the Pt(II) derivatives **3** and **4**.

Finally, the catalytic potential of all the platinum complexes synthesized for the cross dehydrogenative coupling of hydrosilanes with alcohols was briefly investigated (Scheme 8). This catalytic transformation represents nowadays an attractive method for the preparation of useful alkoxy silane reagents,^[29] and it has also gained recent interest in the field of hydrogen storage and production.^[30] The choice of this reaction was motivated by the fact that, despite the large number of catalytic systems that have been developed to date,^[29] those based on platinum are still very scarce,^[31] which is rather surprising given the prominent position that this metal occupies in the field of catalytic hydrosilylation reactions.^[32]



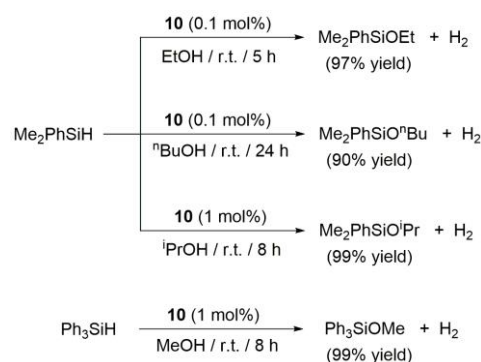
Scheme 8. The catalytic dehydrogenative coupling reaction of hydrosilanes with alcohols.

As model reaction we studied the dehydrogenative coupling of dimethylphenylsilane with methanol, employing the latter directly as a solvent. Thus, in a typical experiment, the corresponding platinum complex (0.1 mol%) was added to a 1 M solution of Me_2PhSiH in MeOH at room temperature, monitoring the course of the reaction by gas chromatography (GC). The results obtained after 40 minutes are collected in Table 1. Of all the complexes synthesized, only $[\text{PtCl}_2\{\kappa^2-(P,N)\text{-}2\text{-Ph}_2\text{PC}_6\text{H}_4\text{CH=NOH}\}]$ (**3**), $(\mu\text{-O})\text{-}[\text{PtCl}\{\kappa^2-(P,N)\text{-}2\text{-Ph}_2\text{PC}_6\text{H}_4\text{CH=NO}\}]_2$ (**5**) and $\text{fac}\text{-}[\text{Pt}(\text{Me}_3\{\kappa^2-(P,N)\text{-}2\text{-Ph}_2\text{PC}_6\text{H}_4\text{CH=NOH}\})]$ (**10**) presented a remarkable reactivity (entries 1, 3 and 6), with the Pt(IV) derivative **10** showing the highest catalytic activity (quantitative formation of the desired methoxydimethyl(phenyl)silane after 40 min.; turnover frequency of 1486 h^{-1}).^[33] Taking into account that in no case Pt(IV) derivatives were considered in previous studies (only Pt(II)^[31a] and Pt(0)^[31b,c] species were tested), this result may be of some relevance for future studies. The low activity found for $[\text{Pt}\{\kappa^2-(P,N)\text{-}2\text{-Ph}_2\text{PC}_6\text{H}_4\text{CH=NOH}\}_2][\text{Cl}]_2$ (**4**) and $[\text{Pt}\{\kappa^2-(P,N)\text{-}2\text{-Ph}_2\text{PC}_6\text{H}_4\text{CH=NO}\}_2\text{H}][\text{Cl}]$ (**8**) is probably related to the steric congestion around the platinum atom in these compounds that prevents the coordination of the silane.^[34] On the other hand, the differences in activity observed between the dinuclear derivatives **5** and **7**, seems to indicate that the activity of the former is associated to the presence of the labile chloride ligands, which can dissociate in the polar reaction medium employed.^[35] Halide dissociation processes, along with the hemilability of the phosphine-oxime ligand, in the less sterically crowded compounds $[\text{PtCl}_2\{\kappa^2-(P,N)\text{-}2\text{-Ph}_2\text{PC}_6\text{H}_4\text{CH=NOH}\}]$ (**3**) and $\text{fac}\text{-}[\text{Pt}(\text{Me}_3\{\kappa^2-(P,N)\text{-}2\text{-Ph}_2\text{PC}_6\text{H}_4\text{CH=NOH}\})]$ (**10**) would explain their superior reactivity (*i.e.* vacant sites for hydrosilane bonding would be in these cases easily generated).

Table 1. Pt-catalyzed dehydrogenative coupling of Me_2PhSiH with MeOH .^[a]

Entry	Catalyst	Conversion [%]	Yield [%] ^[b]	TOF [h^{-1}]
1	3	96	92	1394
2 ^[c]	4	3	3	45
3 ^[d]	5	74	73	1106
4 ^[e]	7	2	2	30
5 ^[f]	8	2	2	30
6	10	99	99	1486

[a] Reactions were performed under Ar atmosphere starting from 1 mmol of Me_2PhSiH (1 M in MeOH). [b] Determined by GC. Differences between GC conversions and yields corresponds to the disiloxane $\text{Me}_2\text{PhSiOSiPhMe}_2$. [c] 34% GC conversion after 24 h. [d] 97% GC conversion after 2 h. [e] 9% GC conversion after 24 h. [f] 7% GC conversion after 24 h.



Scheme 9. Additional cross dehydrogenative coupling reactions catalyzed by the platinum(IV) complex $\text{fac}\text{-}[\text{Pt}(\text{Me}_3\{\kappa^2-(P,N)\text{-}2\text{-Ph}_2\text{PC}_6\text{H}_4\text{CH=NOH}\})]$ (**10**).

We also carried out additional experiments varying the nature of the alcohol and hydrosilane (Scheme 9) employing the most active complex **10**. The results obtained showed an important influence of the steric constraints associated to the substrates in the efficiency of this Pt(IV) catalyst. Thus, although the reactions of dimethylphenylsilane with ethanol and butanol also generated the corresponding alkoxy silanes in high yield (90-97%) using only 0.1 mol% of **10**, longer reaction times were in both cases required (5 and 24 h, respectively). On the other hand, when employing a bulkier secondary alcohol, *i.e.* isopropanol, its reaction with dimethylphenylsilane in the presence of 0.1 mol% **10** could not be completed even after 48 h (79% conversion by GC), an increase in the Pt loading to 1 mol% being required to generate isopropoxydimethyl(phenyl)silane in quantitative yield. A similar fact was observed in the reaction of the bulkier triphenylsilane with methanol to generate methoxytriphenylsilane (99% yield after 8 h with 1 mol% of **10**).

Finally, in order to determine whether the presence of the oxime group vs a more classical imine in the ligand backbone has any effect on the catalytic activity, the dehydrogenative coupling of dimethylphenylsilane with methanol (Table 1) in the presence of complex [PtCl₂{κ²-(*P,N*)-2-Ph₂PC₆H₄CH=N^tBu}] (**11**) (0.1 mol%) was also studied (details on the synthesis and characterization of this complex can be found in the Experimental Section). In this regard, we found that the effectiveness of **11** (97% conversion and 94% yield after 40 min at r.t.) is almost identical to that shown by [PtCl₂{κ²-(*P,N*)-2-Ph₂PC₆H₄CH=NOH}] (**3**) (see entry 1 in Table 1), thus discarding an active participation of the OH group in the catalytic transformation.

Conclusions

In summary, the reactivity of the commercially available ligand 2-(diphenylphosphino)benzaldehyde oxime (**1**) towards the Pt(II) and Pt(IV) precursors [PtCl₂(COD)], [PtMe₂(COD)] and [PtMe₃]₄ has been explored. As a result of this study, new mono- and dinuclear platinum complexes could be obtained in a selective manner, some of them showing catalytic activity in the cross dehydrogenative coupling of hydrosilanes with alcohols. To the best of our knowledge the compounds synthesized here represent the first examples of platinum(II) and platinum(IV) complexes containing a mixed phosphino-oxime/oximate ligand. As commented in the introduction of this article, the chemistry of the hybrid ligand **1** remains to date virtually unexplored. In this regard, as the most noticeable novelty in the field, we have evidenced for the first time the coordination of its oximate anion to a metal center.

Experimental Section

General: All the manipulations were performed under argon atmosphere using vacuum-line and standard Schlenk techniques. Organic solvents were dried by standard methods and distilled under argon before use.^[36] All reagents were obtained from commercial suppliers and used as received, with the exception of complexes [PtCl₂(COD)] (**2**),^[37] [PtMe₂(COD)] (**6**)^[38] and [PtMe₃]₄ (**9**),^[39] and the phosphino-imine ligand 2-Ph₂PC₆H₄CH=N^tBu,^[40] which were prepared following the methods reported in the literature. Elemental analyses and HRMS were provided by the Scientific-Technical Services of the University of Oviedo. The latter were recorded using positive electrospray ionization by the TOF method. Infrared spectra were recorded on a Perkin-Elmer 1720-XFT spectrometer. Conductance measurements were made at room temperature, with ca. 10⁻³ M DMSO solutions, employing a Jenway PCM3 conductometer. GC measurements were performed with a Hewlett-Packard HP6890 equipment using a Supelco Beta-Dex™ 120 column (30 m length; 250 μm diameter). NMR spectra were recorded on Bruker DPX-300 or AV400 instruments. The chemical shift values (δ) are given in parts per million and are referred to the residual peak of the deuterated solvent employed (¹H and ¹³C) or to an external 85% aqueous H₃PO₄ solution (³¹P). DEPT experiments have been carried out for all the compounds reported.

Synthesis of [PtCl₂{κ²-(*P,N*)-2-Ph₂PC₆H₄CH=NOH}] (3**):** A mixture of 2-Ph₂PC₆H₄CH=NOH (**1**) (0.214 g, 0.700 mmol) and [PtCl₂(COD)] (**2**) (0.262 g, 0.700 mmol) and in 20 mL of dichloromethane was stirred overnight at room temperature. The resulting solution was then concentrated under reduced pressure to ca. 5 mL. Addition of hexanes (50 mL) led to the precipitation of a yellow solid, which was washed with hexanes (3 x 10 mL) and dried in vacuo. Yield: 0.348 g (87%). IR (KBr): ν = 3415 (br, OH), 1635 (m, C=N) cm⁻¹. ³¹P{¹H} NMR (CD₂Cl₂, 121 MHz): δ = 1.1 (s, J_{Pt,P} = 3735.0 Hz) ppm. ¹H NMR (CD₂Cl₂, 400 MHz): δ = 11.99 (s, 1 H, OH), 8.53 (s, J_{Pt,H} = 77.6 Hz, 1 H, CH=N), 7.74-7.52 (m, 13 H, CH_{arom}), 7.28 (br s, 1 H, CH_{arom}) ppm. ¹³C{¹H} NMR (CD₂Cl₂, 100 MHz): δ = 147.2 (d, J_{P,C} = 6.1 Hz, J_{Pt,C} = 59.7 Hz, C=N), 135.2 (d, J_{P,C} = 9.1 Hz, CH_{arom}), 134.6 (d, J_{P,C} = 3.7 Hz, J_{Pt,C} = 21.7 Hz, CH_{arom}), 133.9 (d, J_{P,C} = 11.1 Hz, J_{Pt,C} = 30.0 Hz, CH_{arom}), 133.4 (d, J_{P,C} = 13.5 Hz, C_{arom}), 133.2 (d, J_{P,C} = 8.4 Hz, CH_{arom}), 133.1 (d, J_{P,C} = 2.4 Hz, CH_{arom}), 132.2 (d, J_{P,C} = 2.8 Hz, CH_{arom}), 128.8 (d, J_{P,C} = 12.3 Hz, CH_{arom}), 126.6 (d, J_{P,C} = 71.2 Hz, J_{Pt,C} = 24.5 Hz, C_{arom}), 118.4 (d, J_{P,C} = 60.3 Hz, C_{arom}) ppm. Elemental analysis calcd. (%) for C₁₉H₁₆Cl₂NOPt: C 39.95, H 2.82, N 2.45; found: C 40.08, H 2.74, N 2.60. HRMS (ESI): *m/z* 536.0295, [M - Cl]⁺.

Synthesis of [Pt{κ²-(*P,N*)-2-Ph₂PC₆H₄CH=NOH}]₂[Cl]₂ (4**):** A mixture of 2-Ph₂PC₆H₄CH=NOH (**1**) (0.428 g, 1.400 mmol) and [PtCl₂(COD)] (**2**) (0.262 g, 0.700 mmol) and in 30 mL of dichloromethane was stirred overnight at room temperature. The resulting solution was then concentrated under reduced pressure to ca. 5 mL. Addition of hexanes (30 mL) led to the precipitation of a yellow solid, which was recrystallized twice with CH₂Cl₂-hexanes (5:30 mL), washed with hexanes (2 x 10 mL) and dried in vacuo. Yield: 0.509 g (83%). IR (KBr): ν = 3430 (br, OH), 1604 (m, C=N) cm⁻¹. ³¹P{¹H} NMR (CD₂Cl₂, 121 MHz): δ = 6.1 (s, J_{Pt,P} = 3620.6 Hz) ppm. ¹H NMR (CD₂Cl₂, 300 MHz): δ = 14.12 (br s, 2 H, OH), 8.81 (br s, 8 H, CH=N and CH_{arom}), 7.63-7.48 (m, 18 H, CH_{arom}), 6.92 (br s, 4 H, CH_{arom}) ppm. ¹³C{¹H} NMR (CD₂Cl₂, 100 MHz): δ = 152.4 (br s, C=N), 136.3 (br s, CH_{arom}), 134.5 (br s, CH_{arom}), 134.0 (br s, C_{arom}), 133.0 (br s, CH_{arom}), 132.2 (d, J_{P,C} = 4.4 Hz, CH_{arom}), 132.1 (s, CH_{arom}), 131.5 (s, CH_{arom}), 129.0 (br s, CH_{arom}), 124.9 (d, J_{P,C} = 64.4 Hz, C_{arom}), 122.4 (d, J_{P,C} = 57.2 Hz, C_{arom}) ppm. Elemental analysis calcd. (%) for C₃₈H₃₂Cl₂N₂O₂P₂Pt: C 52.07, H 3.68, N 3.20; found: C 51.92, H 3.71, N 3.33. HRMS (ESI): *m/z* 804.1482, [M - H]⁺.

Synthesis of (μ-O)-[PtCl{κ²-(*P,N*)-2-Ph₂PC₆H₄CH=NO}]₂ (5**):** A solution of [PtCl₂{κ²-(*P,N*)-2-Ph₂PC₆H₄CH=NOH}] (**3**) (0.150 g, 0.262 mmol) in 10 mL of dichloromethane was treated at r.t. with Na₂CO₃ (0.278 g, 2.620 mmol) for 20 h. The resulting suspension was then filtered through Kieselguhr, and the filtrate concentrated under vacuum to ca. 2 mL. Addition of hexanes (30 mL) led to the precipitation of a yellow solid, which was washed with hexanes (3 x 5 mL) and dried in vacuo. Yield: 0.110 g (79%). IR (KBr): ν = 1579 (m, C=N) cm⁻¹. ³¹P{¹H} NMR (CD₂Cl₂, 121 MHz): δ = 0.7 (s, J_{Pt,P} = 3859.1 Hz) ppm. ¹H NMR (CD₂Cl₂, 400 MHz): δ = 8.25 (s, J_{Pt,H} = 75.6 Hz, 2 H, CH=N), 7.80-7.75 (m, 8 H, CH_{arom}), 7.61-7.43 (m, 18 H, CH_{arom}), 7.10 (dd, J_{P,H} = 11.2 Hz, J_{H,H} = 8.0 Hz, 2 H, CH_{arom}) ppm. ¹³C{¹H} NMR (CD₂Cl₂, 100 MHz): δ = 141.5 (virtual t, N = 11.0 Hz, C=N), 136.5 (d, J_{P,C} = 13.3 Hz, C_{arom}), 134.2 (d, J_{P,C} = 11.2 Hz, CH_{arom}), 132.4 (d, J_{P,C} = 1.6 Hz, CH_{arom}), 132.3 (d, J_{P,C} = 4.3 Hz, CH_{arom}), 131.8 (d, J_{P,C} = 2.4 Hz, CH_{arom}), 131.7 (d, J_{P,C} = 5.9 Hz, CH_{arom}), 130.3 (d, J_{P,C} = 8.6 Hz, CH_{arom}), 128.5 (d, J_{P,C} = 12.0 Hz, CH_{arom}), 126.7 (d, J_{P,C} = 69.1 Hz, C_{arom}), 118.7 (d, J_{P,C} = 63.5 Hz, C_{arom}) ppm. Elemental analysis calcd. (%) for C₃₈H₃₀Cl₂N₂O₂P₂Pt₂: C 42.67, H 2.83, N 2.62; found: C 42.81, H 2.90, N 2.51. HRMS (ESI): *m/z* 1033.0766, [M - Cl]⁺.

Synthesis of (μ-O)-[PtMe{κ²-(*P,N*)-2-Ph₂PC₆H₄CH=NO}]₂ (7**):** A mixture of [PtMe₂(COD)] (**6**) (0.100 g, 0.300 mmol) and 2-Ph₂PC₆H₄CH=NOH (**1**) (0.091 g, 0.300 mmol) in 15 mL of dichloromethane was stirred overnight at room temperature. The resulting solution was then concentrated under reduced pressure to ca. 5 mL. Addition of hexanes (50 mL) led to the

precipitation of a yellow solid, which was recrystallized twice with CH₂Cl₂-hexanes (5:40 mL), washed with hexanes (3 x 10 mL) and dried in vacuo. Yield: 0.093 g (60%). IR (KBr): $\nu = 1575$ (m, C=N) cm⁻¹. ³¹P{¹H} NMR (CD₂Cl₂, 121 MHz): $\delta = 11.6$ (s, $J_{\text{Pt,P}} = 4412.3$ Hz) ppm. ¹H NMR (CD₂Cl₂, 300 MHz): $\delta = 8.25$ (s, $J_{\text{Pt,H}} = 31.8$ Hz, 2 H, CH=N), 7.73-7.34 (m, 26 H, CH_{arom}), 7.06 (dd, $J_{\text{P,H}} = 10.2$ Hz, $J_{\text{H,H}} = 8.4$ Hz, 2 H, CH_{arom}), 0.02 (d, $J_{\text{P,H}} = 1.8$ Hz, $J_{\text{Pt,H}} = 64.8$ Hz, 6 H, Me) ppm. ¹³C{¹H} NMR (CD₂Cl₂, 100 MHz): $\delta = 143.6$ (virtual t, $N = 9.8$ Hz, C=N), 139.6 (d, $J_{\text{P,C}} = 13.2$ Hz, C_{arom}), 135.9 (d, $J_{\text{P,C}} = 11.5$ Hz, CH_{arom}), 134.0 (d, $J_{\text{P,C}} = 1.0$ Hz, CH_{arom}), 133.2 (d, $J_{\text{P,C}} = 2.1$ Hz, CH_{arom}), 133.1 (d, $J_{\text{P,C}} = 9.4$ Hz, CH_{arom}), 132.8 (d, $J_{\text{P,C}} = 2.4$ Hz, CH_{arom}), 130.8 (d, $J_{\text{P,C}} = 63.7$ Hz, C_{arom}), 130.5 (d, $J_{\text{P,C}} = 8.4$ Hz, CH_{arom}), 130.1 (d, $J_{\text{P,C}} = 11.3$ Hz, CH_{arom}), 124.0 (d, $J_{\text{P,C}} = 60.6$ Hz, C_{arom}), -10.2 (d, $J_{\text{P,C}} = 5.8$ Hz, Me) ppm. Elemental analysis calcd. (%) for C₄₀H₃₆N₂O₂P₂Pt₂: C 46.70, H 3.53, N 2.72; found: C 46.77, H 3.62, N 2.84. HRMS (ESI): m/z 1029.1573, [M + H]⁺.

Synthesis of [Pt(κ^2 -(*P,M*)-2-Ph₂PC₆H₄CH=NO)₂H][Cl] (8): A solution of [Pt(κ^2 -(*P,M*)-2-Ph₂PC₆H₄CH=NOH)₂][Cl]₂ (4) (0.150 g, 0.171 mmol) in 10 mL of dichloromethane was treated at r.t. with Na₂CO₃ (0.181 g, 1.710 mmol) for 20 h. The resulting suspension was then filtered through Kieselguhr, and the filtrate concentrated under vacuum to ca. 2 mL. Addition of hexanes (30 mL) led to the precipitation of a yellow solid, which was recrystallized twice with CH₂Cl₂-hexanes (2:30 mL), washed with hexanes (2 x 5 mL) and dried in vacuo. Yield: 0.105 g (73%). IR (KBr): $\nu = 1741$ (s, O-H-O), 1630 (m, C=N) cm⁻¹. ³¹P{¹H} NMR (CD₂Cl₂, 121 MHz): $\delta = 5.6$ (s, $J_{\text{Pt,P}} = 3273.6$ Hz) ppm. ¹H NMR (CD₂Cl₂, 400 MHz): $\delta = 8.18$ (d, $J_{\text{P,H}} = 8.4$ Hz, $J_{\text{Pt,H}} = 56.0$ Hz, 2 H, CH=N), 7.65-7.30 (m, 26 H, CH_{arom}), 6.85 (dd, $J_{\text{H,H}} = 7.8$ Hz, $J_{\text{P,H}} = 6.0$ Hz, 2 H, CH_{arom}) ppm; O-H-O signal not observed. ¹³C{¹H} NMR (CD₂Cl₂, 100 MHz): $\delta = 150.1$ (br s, C=N), 134.2 (virtual t, $N = 10.2$ Hz, CH_{arom}), 134.0 (virtual t, $N = 25.8$ Hz, C_{arom}), 133.6 (virtual t, $N = 9.2$ Hz, CH_{arom}), 132.8 (s, CH_{arom}), 132.7 (s, CH_{arom}), 133.2 (virtual t, $N = 3.6$ Hz, CH_{arom}), 131.9 (virtual t, $N = 9$ Hz, CH_{arom}), 129.3 (virtual t, $N = 11.6$ Hz, CH_{arom}), 124.9 (d, $J_{\text{P,C}} = 68.6$ Hz, C_{arom}), 121.7 (d, $J_{\text{P,C}} = 62.4$ Hz, C_{arom}) ppm. Elemental analysis calcd. (%) for C₃₈H₃₁N₂O₂P₂ClPt: C 54.33, H 3.72, N 3.33; found: C 54.25, H 3.80, N 3.42. HRMS (ESI): m/z 804.1483, [M]⁺.

Synthesis of fac-[PtMe₃(κ^2 -(*P,M*)-2-Ph₂PC₆H₄CH=NOH)] (10): A mixture of 2-Ph₂PC₆H₄CH=NOH (1) (0.125 g, 0.410 mmol) and [PtMe₃]₄ (9) (0.150 g, 0.102 mmol) and in 30 mL of dichloromethane was stirred overnight at room temperature. The resulting solution was then concentrated under reduced pressure to ca. 5 mL. Addition of hexanes (30 mL) led to the precipitation of a yellow solid, which was recrystallized twice with CH₂Cl₂-hexanes (5:30 mL), washed with hexanes (2 x 10 mL) and dried in vacuo. Yield: 0.228 g (83%). IR (KBr): $\nu = 3484$ (br, OH), 1625 (m, C=N) cm⁻¹. ³¹P{¹H} NMR (CD₂Cl₂, 121 MHz): $\delta = -0.2$ (s, $J_{\text{Pt,P}} = 1208.9$ Hz) ppm. ¹H NMR (CD₂Cl₂, 400 MHz): $\delta = 13.05$ (br s, 1 H, OH), 8.29 (s, $J_{\text{Pt,H}} = 19.2$ Hz, 1 H, CH=N), 7.62-7.24 (m, 13 H, CH_{arom}), 7.06 (br s, 1 H, CH_{arom}), 1.52 (s, $J_{\text{Pt,H}} = 59.6$ Hz, 3 H, Me), 1.33 (s, $J_{\text{Pt,H}} = 80.4$ Hz, 3 H, Me), 1.06 (s, $J_{\text{Pt,H}} = 64.8$ Hz, 3 H, Me) ppm. ¹³C{¹H} NMR (CD₂Cl₂, 100 MHz): $\delta = 151.5$ (s, C=N), 135.5 (d, $J_{\text{P,C}} = 9.7$ Hz, CH_{arom}), 134.5 (s, CH_{arom}), 134.1 (d, $J_{\text{P,C}} = 8.6$ Hz, CH_{arom}), 133.9 (d, $J_{\text{P,C}} = 20.8$ Hz, C_{arom}), 133.6 (d, $J_{\text{P,C}} = 9.5$ Hz, CH_{arom}), 132.2 (d, $J_{\text{P,C}} = 5.8$ Hz, CH_{arom}), 131.5 (s, CH_{arom}), 131.2 (d, $J_{\text{P,C}} = 1.0$ Hz, CH_{arom}), 130.9 (s, CH_{arom}), 128.7 (d, $J_{\text{P,C}} = 9.2$ Hz, CH_{arom}), 128.1 (d, $J_{\text{P,C}} = 9.9$ Hz, CH_{arom}), 127.5 (d, $J_{\text{P,C}} = 65.6$ Hz, C_{arom}), 127.1 (d, $J_{\text{P,C}} = 63.6$ Hz, C_{arom}), 125.6 (d, $J_{\text{P,C}} = 39.8$ Hz, $J_{\text{Pt,C}} = 26.3$ Hz, C_{arom}), 8.9 (s, $J_{\text{Pt,C}} = 643.7$ Hz, Me), 7.8 (s, $J_{\text{Pt,C}} = 535.7$ Hz, Me), 6.6 (s, $J_{\text{Pt,C}} = 535.8$ Hz, Me) ppm. Elemental analysis calcd. (%) for C₂₂H₂₅INOPPt: C 39.30, H 3.75, N 2.08; found: C 39.41, H 3.62, N 2.15. HRMS (ESI): m/z 533.0952, [M - I - 2Me + H₂O]⁺.

Synthesis of [PtCl₂(κ^2 -(*P,M*)-2-Ph₂PC₆H₄CH=NⁱBu)] (11): A mixture of 2-Ph₂PC₆H₄CH=NⁱBu (0.145 g, 0.420 mmol) and [PtCl₂(COD)] (2) (0.150 g, 0.400 mmol) and in 10 mL of dichloromethane was stirred overnight at

room temperature. The resulting solution was then concentrated under reduced pressure to ca. 2 mL. Addition of hexanes (20 mL) led to the precipitation of a yellow solid, which was washed with hexanes (3 x 5 mL) and dried in vacuo. Yield: 0.193 g (79%). IR (KBr): $\nu = 1612$ (m, C=N) cm⁻¹. ³¹P{¹H} NMR (CD₂Cl₂, 121 MHz): $\delta = 7.1$ (s, $J_{\text{Pt,P}} = 3775.3$ Hz) ppm. ¹H NMR (CD₂Cl₂, 400 MHz): $\delta = 8.37$ (s, $J_{\text{Pt,H}} = 99.3$ Hz, 1 H, CH=N), 7.74-7.52 (m, 13 H, CH_{arom}), 7.88 (br s, 1 H, CH_{arom}), 1.51 (s, 9 H, CH₃) ppm. ¹³C{¹H} NMR (CD₂Cl₂, 100 MHz): $\delta = 164.8$ (d, $J_{\text{P,C}} = 7.0$ Hz, C=N), 138.9 (d, $J_{\text{P,C}} = 13.0$ Hz, C_{arom}), 134.9-134.0 (m, CH_{arom} and C_{arom}), 133.3 (d, $J_{\text{P,C}} = 7.7$ Hz, CH_{arom}), 132.3 (d, $J_{\text{P,C}} = 1.7$ Hz, CH_{arom}), 132.2 (d, $J_{\text{P,C}} = 8.4$ Hz, CH_{arom}), 131.5 (d, $J_{\text{P,C}} = 4.2$ Hz, CH_{arom}), 122.9 (d, $J_{\text{P,C}} = 61.4$ Hz, C_{arom}), 69.8 (s, C(CH₃)₃), 31.9 (s, C(CH₃)₃) ppm. Elemental analysis calcd. (%) for C₂₃H₂₄Cl₂NPt: C 45.18, H 3.96, N 2.29; found: C 45.23, H 4.01, N 2.37.

General procedure for the catalytic cross dehydrogenative coupling of hydrosilanes with alcohols:

The corresponding hydrosilane (1 mmol), alcohol (1 mL) and platinum catalyst (0.0005 or 0.01 mmol; 0.1-1 mol%) were introduced into a Teflon-capped sealed tube, and the reaction mixture stirred at room temperature for the indicated time (see Table 1 and Scheme 9). The course of the reaction was monitored regularly taking samples of ca. 10 μ L which, after dilution with CH₂Cl₂, were analyzed by GC. The identity of the alkoxy silanes formed was assessed by comparison of their NMR data with those reported in the literature (copies of the ¹H and ¹³C{¹H} NMR spectra of the products obtained after purification by flash chromatography are included in the Supporting Information).

X-Ray crystal structure determination of complexes 3, 4, 7 and 10:

Crystals of **3**, **4**, **7** and **10** suitable for X-ray diffraction analysis were obtained in all the cases by slow diffusion of hexanes into a saturated solution of the complex in a dichloromethane/methanol mixture (3:1 v/v). The most relevant crystal and refinement data are collected in Table 2. In all the cases, data collection was performed with a Rigaku-Oxford Diffraction Xcalibur Onyx Nova single crystal diffractometer using Cu-K α radiation ($\lambda = 1.5418$ Å). Images were collected at a fixed crystal-detector distance of 62 mm, using the oscillation method with 1.30° oscillation for **3** and **10** and 1.10° for **4** and **7**, and 2.00-4.00 s variable exposure time per image for **3**, 3.50-7.00 s for **4**, 2.00-5.00 s for **7** and 4.00-12.50 s for **10**. Data collection strategy was calculated with the program CrysAlisPro.^[41] Data reduction and cell refinement were also performed with the program CrysAlisPro.^[41] An empirical absorption correction was applied using the SCALE3 ABSPACK algorithm as implemented in the program CrysAlisPro.^[41] All the structures were solved by Patterson interpretation and phase expansion using DIRDIF2008.^[42] Isotropic least-squares refinements on F^2 using SHELXL2014^[43] were performed. During the final stages of the refinements, all the positional and anisotropic displacement parameters of all non-H atoms were refined (except C18 in complex **3**).

For **3**, hydrogen atoms bonded to C1 and O1 were unequivocally located using a difference electron density Fourier synthesis and their coordinates and isotropic displacement parameters were freely refined. The rest of H atoms were geometrically located, their coordinates refined riding on their parent atoms, and their isotropic displacement parameters automatically replaced with -1.2. SHELXL2014^[43] suggested splitting C18 into two positions. Accordingly, C18 was isotropically refined using the two possible sites suggested by SHELXL2014^[43] and the final occupation factors of the two components were 54.6 and 45.4%.

For **4**, two independent molecules of the complex and four molecules of methanol were found in the asymmetric unit. Hydrogen atoms bonded to C1A, O1A, C1B and O1B were clearly located using a difference electron density Fourier synthesis and their coordinates and isotropic displacement parameters were freely refined. The same situation occurred with the analogous hydrogen atoms of the second molecule of the complex. The rest of H atoms (in both molecules) were geometrically located, their coordinates refined riding on their parent atoms, and their isotropic

displacement parameters automatically replaced with -1.2. The hydrogen atoms of the methanol molecules were also geometrically located. The final positions of these H atoms were obtained after a rotating group refinement (the initial torsion angle is derived from a difference Fourier synthesis), their isotropic displacement parameters were automatically replaced with -1.5.

For **7**, there is only one half of the complex in the asymmetric unit of the crystal (that contains, in addition, one molecule of methanol), a twofold axis generating the other half. The hydrogen atom bonded to C1 was

located using a difference electron density Fourier synthesis. Its coordinates were freely refined, but its isotropic displacement parameter was replaced with -1.2 (otherwise, an impossible non-positive definite value is generated). The rest of H atoms in the complex were geometrically located, their coordinates refined riding on their parent atoms, and their isotropic displacement parameters automatically replaced with -1.2 (-1.5 for those on the C20 carbon atom). The final positions of the hydrogen atoms on C20 were obtained after a rotating group refinement (the initial torsion angle is derived from a difference Fourier synthesis).

Table 2. Crystal data and structure refinement details for compounds **3**, **4**, **7** and **10**.

	3	4	7	10
Chemical formula	C ₁₉ H ₁₆ Cl ₂ NOPPt	C ₃₈ H ₃₂ Cl ₂ N ₂ O ₂ P ₂ Pt·2MeOH	C ₄₀ H ₃₆ N ₂ O ₂ P ₂ Pt ₂ ·2MeOH	C ₂₂ H ₂₅ INOPPt
Molecular mass	571.29	940.67	1092.91	672.39
T [K]	145(2)	145(2)	150(2)	150(2)
Wavelength [Å]	1.54184	1.54184	1.54184	1.54184
Crystal system	Monoclinic	Triclinic	Orthorhombic	Monoclinic
Space group	P2 ₁ /n	P-1	P2 ₁ 2 ₁ 2	P2 ₁ /c
Crystal size [mm]	0.18 x 0.06 x 0.05	0.18 x 0.12 x 0.09	0.28 x 0.07 x 0.04	0.14 x 0.05 x 0.03
a [Å]	9.0342(2)	14.2374(5)	15.0140(3)	9.5525(3)
b [Å]	15.9840(2)	14.9594(6)	14.4502(3)	7.7081(3)
c [Å]	13.1625(2)	19.6876(6)	8.8870(2)	29.2219(8)
α [°]	90	69.540(3)	90	90
β [°]	90.826(2)	83.690(3)	90	91.179(3)
γ [°]	90	73.287(3)	90	90
Z	4	4	2	4
V [Å ³]	1900.51(5)	3762.4(2)	1928.09(7)	2151.2(1)
ρ _{calcd} [g cm ⁻³]	1.997	1.661	1.883	2.076
μ [mm ⁻¹]	17.249	9.443	14.515	24.256
F(000)	1088	1872	1056	1272
θ range [°]	4.35-69.61	3.24-69.82	4.25-69.50	3.02-69.62
Index ranges	-10 ≤ h ≤ 9 -19 ≤ k ≤ 17 -15 ≤ l ≤ 15	-16 ≤ h ≤ 17 -17 ≤ k ≤ 17 -23 ≤ l ≤ 23	-17 ≤ h ≤ 18 -17 ≤ k ≤ 16 -10 ≤ l ≤ 8	-9 ≤ h ≤ 11 -8 ≤ k ≤ 9 -29 ≤ l ≤ 35
Completeness to θ _{max} [%]	99.8%	99.7%	99.9%	99.7%
No. of data collected	9045	13880	9540	10303
No. of unique data	3502 (R _{int} = 0.0272)	12452 (R _{int} = 0.0349)	3468 (R _{int} = 0.0343)	3973 (R _{int} = 0.0466)
No. parameters/restraints	234/0	959/0	241/0	252/0
Refinement method		Full-matrix least-squares on F ²		
Goodness of fit on F ²	1.034	1.039	1.056	1.044
Weight function (a, b)	0.0307, 0.0000	0.0404, 0.5120	0.0346, 2.2252	0.0638, 0.0000
R [F ² > 2σ(F ²)] ^[a]	0.0234	0.0289	0.0251	0.0413
wR(F ²) [F ² > 2σ(F ²)] ^[a]	0.0548	0.0720	0.0613	0.1036
R (all data)	0.0272	0.0337	0.0271	0.0477
wR(F ²) (all data)	0.0571	0.0751	0.0635	0.1098
Largest diff peak and hole [e.Å ⁻³]	0.596, -1.315	1.138, -1.348	0.779, -0.936	1.712, -1.398

[a] $R = \sum |F_o - F_c| / \sum F_o$; $wR(F^2) = \{\sum [w(F_o^2 - F_c^2)^2] / \sum [w(F_o^2)^2]\}^{1/2}$.

For **10**, the hydrogen atom bonded to C1 was unequivocally located using a difference electron density Fourier synthesis and their coordinates and isotropic displacement parameter were freely refined. The rest of H atoms (including that bonded to O1) were geometrically located, their coordinates, refined riding on their parent atoms, and their isotropic displacement parameters automatically replaced with -1.2 (-1.5 for those on the C20, C21, C22 and O1 atoms). The final positions of the hydrogen

atoms on C20, C21, C22 and O1 were obtained after a rotating group refinement (the initial torsion angle is derived from a difference Fourier synthesis).

The function minimized was $\{\sum [\omega(F_o^2 - F_c^2)^2] / \sum [\omega(F_o^2)^2]\}^{1/2}$ where $\omega = 1/[\sigma^2(F_o^2) + (aP)^2 + bQ]$ (a and b values are collected in Table 2) with $\sigma(F_o^2)$

from counting statistics and $P = [\text{Max}(F_o^2, 0) + 2F_c^2]/3$. The crystallographic plots were made with DIAMOND.^[44]

CCDC 1830710 (for **3**), 1830711 (for **4**), 1830712 (for **7**) and 1830713 (for **10**) contain the supplementary crystallographic data for this paper. These data can be obtained free of charge from The Cambridge Crystallographic Data Centre.

Acknowledgements

This work was supported by the Spanish MINECO (projects CTQ2016-75986-P, CTQ2016-76267-P and CTQ2016-81797-REDC), the Gobierno del Principado de Asturias (project GRUPIN14-006) and the Junta de Andalucía (project FQM-2126). J.F. thanks MINECO and ESF for the award of a Juan de la Cierva contract (IJC1-2014-19174).

Keywords: Hybrid ligands • Phosphino-oxime • Phosphino-oximate • Platinum • Silanes

- [1] See, for example: a) P. Espinet, K. Soulantica, *Coord. Chem. Rev.* **1999**, 193-195, 499-556; b) P. Braunstein, *J. Organomet. Chem.* **2004**, 689, 3953-3967; c) J. G. Fierro-Arias, R. Redón, J. J. García, S. Hernández-Ortega, R. A. Toscano, *J. Mol. Catal. A: Chem.* **2005**, 233, 17-27; d) G. Ríos-Moreno, R. A. Toscano, R. Redón, H. Nakano, Y. Okuyama, D. Morales-Morales, *Inorg. Chim. Acta* **2005**, 358, 303-309; e) J. Wassenaar, J. N. H. Reek, *Org. Biomol. Chem.* **2011**, 9, 1704-1713; f) W.-H. Zhang, S. W. Chien, T. S. A. Hor, *Coord. Chem. Rev.* **2011**, 255, 1991-2024; g) Y. Li, M.-H. Xu, *Chem. Commun.* **2014**, 50, 3771-3782; h) J. García-Álvarez, S. E. García-Garrido, V. Cadierno, *J. Organomet. Chem.* **2014**, 751, 792-808; i) Š. Toma, J. Csizmadiová, M. Mečiarová, R. Šebesta, *Dalton Trans.* **2014**, 43, 16557-16579; j) V. R. Landaeta, R. E. Rodríguez-Lugo, *J. Mol. Catal. A: Chem.* **2017**, 426, 316-325; k) P. Štěpnička, *Coord. Chem. Rev.* **2017**, 353, 223-246.
- [2] For selected reviews on hemilabile ligands, see: a) A. Bader, E. Lindner, *Coord. Chem. Rev.* **1991**, 108, 27-110; b) C. S. Slone, D. A. Weinberger, C. A. Mirkin, *Prog. Inorg. Chem.* **1999**, 48, 233-350; c) P. Braunstein, F. Naud, *Angew. Chem.* **2001**, 113, 702-722; *Angew. Chem. Int. Ed.* **2001**, 40, 680-699; d) M. Bassetti, *Eur. J. Inorg. Chem.* **2006**, 4473-4482; e) S. A. Angell, C. W. Rogers, Y. Zhang, M. O. Wolf, W. E. Jones Jr., *Coord. Chem. Rev.* **2006**, 250, 1829-1841; f) F. Y. Kwong, A. S. C. Chan, *Synlett* **2008**, 1440-1448; g) J. I. van der Vlugt, *Eur. J. Inorg. Chem.* **2012**, 363-375.
- [3] For selected recent works with this type of ligands, see: a) E. Badetti, G. Franc, J.-P. Majoral, A.-M. Caminade, R. M. Sebastián, M. Moreno-Mañas, *Eur. J. Org. Chem.* **2011**, 1256-1265; b) T. Inami, S. Sako, T. Kurahashi, S. Matsubara, *Org. Lett.* **2011**, 13, 3837-3839; c) S. Sako, T. Kurahashi, S. Matsubara, *Chem. Commun.* **2011**, 47, 6150-6152; d) T. F. Vaughan, D. J. Koedyk, J. L. Spencer, *Organometallics* **2011**, 30, 5170-5180; e) H. Lei, A. M. Royer, T. B. Rauchfuss, D. Gray, *Organometallics* **2012**, 31, 6408-6414; f) D. A. Rooke, E. M. Ferreira, *Org. Lett.* **2012**, 14, 338-341; g) B. C. E. Makhubela, A. Jardine, G. S. Smith, *Green Chem.* **2012**, 14, 338-347; h) Y. Li, F. Liang, R. Wu, Q. Li, Q.-R. Wang, Y.-C. Xu, L. Jiang, *Synlett* **2012**, 23, 1805-1808; i) H. Chiririwa, J. R. Moss, D. Hendricks, G. S. Smith, R. Meijboom, *Polyhedron* **2013**, 49, 29-35; j) W. M. Motswainyana, M. O. Onani, O. M. Madiehe, M. Saibu, N. Thovhogi, R. A. Lalancette, *J. Inorg. Biochem.* **2013**, 129, 112-118; k) M. K. Yilmaz, B. Güzel, *Appl. Organomet. Chem.* **2014**, 28, 529-536; l) M. Tristany, R. Laurent, H. Dib, L. Gonsalvi, M. Peruzzini, J.-P. Majoral, A.-M. Caminade, *Inorg. Chim. Acta* **2014**, 409, 121-126; m) L. Maqeda, B. C. E. Makhubela, G. S. Smith, *Polyhedron* **2015**, 91, 128-135; n) T. Traut-Johnstone, S. Kanyanda, F. H. Kriel, T. Viljoen, P. D. R. Kotze, W. E. van Xyl, J. Coates, D. J. G. Rees, M. Meyer, R. Hewer, D. B. G. Williams, *J. Inorg. Biochem.* **2015**, 145, 108-120; o) W.-Y. Chu, C. P. Richers, E. R. Kahle, T. B. Rauchfuss, F. Arrigoni and G. Zampella, *Organometallics* **2016**, 35, 2782-2792.
- [4] Compound **1** was synthesized for the first time in 1993 through the reaction 2-(diphenylphosphino)benzaldehyde with hydroxylamine hydrochloride: A. Nikitidis, C. Andersson, *Phosphorus, Sulfur Silicon Relat. Elem.* **1993**, 78, 141-152.
- [5] Compound **1** can be purchased at different chemical suppliers at an average price of about 50 €/g.
- [6] In general, hybrid phosphino-oxime ligands are uncommon in the literature: a) K. Park, P. O. Lagaditis, A. J. Lough, R. H. Morris, *Inorg. Chem.* **2013**, 52, 5448-5456; b) G. C. Dickmu, N. J. Korte, I. P. Smoliakova, *J. Organomet. Chem.* **2015**, 797, 13-20; c) J. E. Kukowski, V. A. Stepanova, I. P. Smoliakova, *J. Organomet. Chem.* **2017**, 830, 155-166.
- [7] For some review articles covering the coordination chemistry of oximes and their oximate anions, see: a) A. Chakravorty, *Coord. Chem. Rev.* **1974**, 13, 1-46; b) V. Y. Kukushkin, D. Tudela, A. J. L. Pombeiro, *Coord. Chem. Rev.* **1996**, 156, 333-362; c) V. Y. Kukushkin, A. J. L. Pombeiro, *Coord. Chem. Rev.* **1999**, 181, 147-175; d) A. G. Smith, P. A. Tasker, D. J. White, *Coord. Chem. Rev.* **2003**, 241, 61-85; e) P. Chaudhuri, *Coord. Chem. Rev.* **2003**, 243, 143-190; f) C. J. Milios, T. C. Stamatatos, S. P. Perlepes, *Polyhedron* **2006**, 25, 134-194; g) D. A. Alonso, C. Nájera, *Chem. Soc. Rev.* **2010**, 39, 2891-2902; h) D. S. Bolotin, N. A. Bokach, V. Y. Kukushkin, *Coord. Chem. Rev.* **2016**, 313, 62-93; i) D. S. Bolotin, N. A. Bokach, M. Y. Demakova, V. Y. Kukushkin, *Chem. Rev.* **2017**, 117, 13039-13122.
- [8] See, for example: a) A. M. Royer, T. B. Rauchfuss, D. L. Gray, *Organometallics* **2010**, 29, 6763-6768; b) A. Bartoszewicz, R. Marcos, S. Sahoo, A. K. Inge, X. Zou, B. Martín-Matute, *Chem. Eur. J.* **2012**, 18, 14510-14519; c) R. Kawahara, K. Fujita, R. Yamaguchi, *J. Am. Chem. Soc.* **2012**, 134, 3643-3646; d) S. Musa, S. Fronton, L. Vaccaro, D. Gelman, *Organometallics* **2013**, 32, 3069-3073; e) W.-H. Wang, J. T. Muckerman, E. Fujita, Y. Himeda, *ACS Catal.* **2013**, 3, 856-860; f) Y. Suna, M. Z. Ertem, W.-H. Wang, H. Kambayashi, Y. Manaka, J. T. Muckerman, E. Fujita, Y. Himeda, *Organometallics* **2014**, 33, 6519-6530; g) G. Zeng, S. Sakaki, K. Fujita, H. Sano, R. Yamaguchi, *ACS Catal.* **2014**, 4, 1010-1020; h) B. Saha, S. M. W. Rahaman, P. Daw, G. Sengupta, J. K. Bera, *Chem. Eur. J.* **2014**, 20, 6542-6551; i) P. Qu, C. Sun, J. Ma, F. Li, *Adv. Synth. Catal.* **2014**, 356, 447-459; j) E. Tomás-Mendivil, V. Cadierno, M. I. Menéndez, R. López, *Chem. Eur. J.* **2015**, 21, 16874-16886; k) A. Bartoszewicz, G. C. Miera, R. Marcos, P.-O. Norrby, B. Martín-Matute, *ACS Catal.* **2015**, 5, 3704-3716; l) R. Wang, H. Fan, W. Zhao, F. Li, *Org. Lett.* **2016**, 18, 3558-3561; m) R. González-Fernández, P. Crochet, V. Cadierno, M. I. Menéndez, R. López, *Chem. Eur. J.* **2017**, 23, 15210-15221; n) G. G. Miera, E. Martínez-Castro, B. Martín-Matute, *Organometallics* **2018**, 37, 636-644; o) R. González-Fernández, P. Crochet, V. Cadierno, *ChemistrySelect* **2018**, 3, 4324-4329.
- [9] L. Menéndez-Rodríguez, E. Tomás-Mendivil, J. Francos, C. Nájera, P. Crochet, V. Cadierno, *Catal. Sci. Technol.* **2015**, 5, 3754-3761.
- [10] J. Francos, L. Menéndez-Rodríguez, E. Tomás-Mendivil, P. Crochet, V. Cadierno, *RSC Adv.* **2016**, 6, 39044-39052.
- [11] a) L. Xu, D. Zhu, F. Wu, R. Wang, B. Wan, *Tetrahedron* **2005**, 61, 6553-6560; b) D. Zhu, L. Xu, F. Wu, B. Wan, *Tetrahedron Lett.* **2006**, 47, 5781-5784.
- [12] L. Xu, D. Zhu, F. Wu, R. Wang, B. Wan, *J. Mol. Catal. A: Chem.* **2005**, 237, 210-214.
- [13] See, for example: a) H.-B. Song, Z.-Z. Zhang, T. C. W. Mak, *Polyhedron* **2002**, 21, 1043-1050; b) H. Chiririwa, R. Meijboom, *Acta Cryst.* **2011**, E67, m1496; c) H. Chiririwa, R. Meijboom, *Acta Cryst.* **2011**, E67, m1497; d) H. Chiririwa, A. Muller, *Acta Cryst.* **2012**, E68, m116-m117; e) P.-D. St-Coeur, S. Kinley, C. M. Vogels, A. Decken, P. Morin Jr., S. A. Westcott, *Can. J. Chem.* **2017**, 95, 207-213.

- [14] See, for example: a) S. Otto, A. Chanda, P. V. Samuleev, A. D. Ryabov, *Eur. J. Inorg. Chem.* **2006**, 2561-2565; b) Y. Y. Scaffidi-Domianello, A. A. Legin, M. A. Jakupec, A. Roller, V. Y. Kukushkin, M. Galanski, B. K. Keppler, *Inorg. Chem.* **2012**, *51*, 7153-7163; c) E. Y. Bulatov, T. G. Chulkova, I. A. Boyarskaya, V. Y. Kondratiev, M. Haukka, V. Y. Kukushkin, *J. Mol. Struct.* **2014**, *1068*, 176-181; d) D. B. Dell'Amico, M. Colalillo, L. Labella, F. Marchetti, S. Samaritani, *Inorg. Chim. Acta* **2018**, *470*, 181-186.
- [15] Metal-bound chlorine atoms are well-known H-bond acceptors: G. Aullón, D. Bellamy, L. Brammer, E. A. Bruton, A. G. Orpen, *Chem. Commun.* **1998**, 653-654.
- [16] a) G. A. Jeffrey, *An Introduction to Hydrogen Bonding*, Oxford University Press, Oxford, **1997**; b) T. Steiner, *Angew. Chem.* **2002**, *114*, 50-80; *Angew. Chem. Int. Ed.* **2002**, *41*, 48-76.
- [17] a) To the best of our knowledge, similar platinum(II) complexes derived from phosphino-imines 2-Ph₂PC₆H₄CH=NR (R = aryl or alkyl group; **A** in Figure 1), have not been described to date in the literature; b) *Cis* arrangement of the diphenylphosphino groups has also been observed in the X-ray crystal structures of the related aminophosphine-Pt(II) complexes [Pt{κ²-(*P,N*)-2-Ph₂P(CH₂)_nNH₂}_2][Cl]₂ (n = 2, 3) and [Pt{κ²-(*P,N*)-2-Ph₂P(CH₂)₂NHMe}_2][HCl]₂ described by Sadler and co-workers: A. Habtemariam, B. Watchman, B. S. Potter, R. Palmer, S. Parsons, A. Parkin, P. J. Sadler, *J. Chem. Soc., Dalton Trans.* **2001**, 1306-1318.
- [18] Also of note is that, in the crystal structure of **4**, the chloride anions establish hydrogen-bonds with the OH groups of the phosphino-oxime ligands and the methanol solvation molecules leading to an extended 3D network (details are given in the Supporting Information file).
- [19] Molar conductivities of 1:1 and 2:1 type electrolytes in DMSO solution usually fall within the ranges 20-40 and 70-90 Ω⁻¹·cm²·mol⁻¹, respectively. See, for example: a) C. Atlani, J.-C. Justice, *J. Solution Chem.* **1975**, *4*, 955-963; b) A. Apelblat, *J. Solution Chem.* **2011**, *40*, 1234-1257.
- [20] Oximate-platinum(II) complexes, as well as oxime-platinum(II) derivatives, have gained enormous interest in recent years as potential anticancer drugs. See, for example, reference 14b and: a) A. G. Quiroga, L. Cubo, E. de Blas, P. Aller, C. Navarro-Ranninger, *J. Inorg. Biochem.* **2007**, *101*, 104-110; b) S. Zorbas-Seifried, M. A. Jakupec, N. V. Kukushkin, M. Groessel, C. G. Hartinger, O. Semenova, H. Zorbas, V. Y. Kukushkin, B. K. Keppler, *Mol. Pharmacol.* **2007**, *71*, 357-365; c) Y. Y. Scaffidi-Domianello, K. Meelich, M. A. Jakupec, V. B. Arion, V. Y. Kukushkin, M. Galanski, B. K. Keppler, *Inorg. Chem.* **2010**, *49*, 5669-5678; d) Y. Y. Scaffidi-Domianello, A. A. Legin, M. A. Jakupec, V. B. Arion, V. Y. Kukushkin, M. Galanski, B. K. Keppler, *Inorg. Chem.* **2011**, *50*, 10673-10681; e) K. Ossipov, Y. Y. Scaffidi-Domianello, I. F. Seregina, M. Galanski, B. K. Keppler, A. R. Timerbaev, M. A. Bolshov, *J. Inorg. Biochem.* **2014**, *137*, 40-45; f) D. S. Bolotin, M. Y. Demakova, A. A. Legin, V. V. Suslonov, A. A. Nazarov, M. A. Jakupec, B. K. Keppler, V. Y. Kukushkin, *New J. Chem.* **2017**, *41*, 6840-6848; g) D. B. D. Amico, M. Colalillo, L. D. Via, M. D. Acqua, A. N. García-Argáez, M. Hyeraci, L. Labella, F. Marchetti, S. Samaritani, *Eur. J. Inorg. Chem.* **2018**, 1589-1594.
- [21] The platinum atoms feature a distorted square planar coordination, with maximum deviations from the mean PtPNOC planes of 0.319(5) Å for the nitrogen atoms.
- [22] See, for example: G. K. Anderson, *Comprehensive Organometallic Chemistry II* (Eds.: E. W. Abel, F. G. A. Stone, G. Wilkinson), Pergamon Press, Oxford, **1995**, vol. 9, pp. 431-531.
- [23] All attempts to promote the double deprotonation of complex **4** by increasing the temperature, the reaction time or the strength of the base employed (KOH in THF) failed.
- [24] The proposed -N-O··H··O-N- interaction is present in the well-known cobaloximes for which detailed studies of their IR spectra have been performed. See, for example: R. Dreos, S. Geremia, L. Randaccio, P. Siega, *Properties, Structure and Reactivity of Cobaloximes*, in *PATAI's Chemistry of Functional Groups*, John Wiley & Sons, Chichester, **2010**.
- [25] a) The reactivity of [PtMe₃]₄ (**9**) towards phosphino-imines **A** (Figure 1) remains almost unexplored. Thus, the only precedents found in the literature are the reactions of **9** with optically pure (*R*)- and (*S*)-2-Ph₂PC₆H₄CH=NCH(Me)Ph to afford diastereomeric mixtures of *fac*-[PtMe₃{κ²-(*P,N*)-2-Ph₂PC₆H₄CH=NCH(Me)Ph}] due to the chirality of the metal center: P. Ramírez, R. Contreras, M. Valderrama, D. Boys, *J. Organomet. Chem.* **2006**, *691*, 491-498; b) To the best of our knowledge, no reactions of [PtMe₃]₄ (**9**) with oxime-based ligands have been reported to date.
- [26] Complex **10** is perfectly stable in solution for long periods at room temperature, but it evolves into a complicated mixture of uncharacterized products upon heating. Apart from the potential deprotonation of the oxime by the methyl ligands, we do not rule out that reductive elimination processes are also taking place at high temperature, as observed by Valderrama and co-workers for the related complexes *fac*-[PtMe₃{κ²-(*P,N*)-2-Ph₂PC₆H₄CH=NCH(Me)Ph}]. See, reference 25a and: P. Ramírez, R. Contreras, M. Valderrama, D. Carmona, F. J. Lahoz, A. I. Balana, *J. Organomet. Chem.* **2008**, *693*, 349-356.
- [27] As expected, a lower J_{Pt,P} coupling constant in comparison to the previous examples was in this case observed (1208.9 Hz). It is well-known that the oxidation state of the metal influences the magnitude of the metal-phosphorus coupling constants, following in the case of platinum the order Pt(0) > Pt(II) > Pt(IV): P. S. Pregosin, R. W. Kunz, ³¹P and ¹³C NMR of Transition Metal Phosphine Complexes, Springer-Verlag, Berlin, **1979**, pp. 16-46.
- [28] See, for example, reference 25a and: a) B. N. Ghosh, M. Lahtinen, E. Kalenius, P. Mal, K. Rissanen, *Cryst. Growth Des.* **2016**, *16*, 2527-2534; b) B. N. Ghosh, S. Schlecht, A. Bauzá, A. Frontera, *New J. Chem.* **2017**, *41*, 3498-3507.
- [29] For a recent review article on the catalytic formation of silicon-heteroatom bonds, covering the alcoholysis of hydrosilanes, see: K. Kuciński, G. Hreczycho, *ChemCatChem* **2017**, *9*, 1868-1885.
- [30] See, for example: a) W. Sattler, G. Parkin, *J. Am. Chem. Soc.* **2012**, *134*, 17462-17465; b) S. Rommel, L. Hettmanczyk, J. E. M. N. Klein, B. Plietker, *Chem. Asian J.* **2014**, *9*, 2140-2147; c) M. Aliaga-Lavrijsen, M. Iglesias, A. Cebollada, K. Garcés, N. García, P. J. S. Miguel, F. J. Fernández-Álvarez, J. J. Pérez-Torrente, L. A. Oro, *Organometallics* **2015**, *34*, 2378-2385; d) D. Ventura-Espinosa, A. Carretero-Cerdán, M. Baya, H. García, J. A. Mata, *Chem. Eur. J.* **2017**, *23*, 10815-10821; e) D. Ventura-Espinosa, S. Sabater, A. Carretero-Cerdán, M. Baya, J. A. Mata, *ACS Catal.* **2018**, *8*, 2558-2566.
- [31] a) W. Caseri, P. S. Pregosin, *Organometallics* **1988**, *7*, 1373-1380; b) K. D. Safa, Y. M. Oskoei, *J. Organomet. Chem.* **2010**, *695*, 505-511; c) J.-X. Xu, M.-Y. Chen, Z.-J. Zheng, J. Cao, Z. Xu, Y.-M. Cui, L.-W. Xu, *ChemCatChem* **2017**, *9*, 3111-3116.
- [32] For some selected reviews, see: a) L. N. Lewis, J. Stein, Y. Gao, R. E. Colborn, G. Hutchins, *Platinum Metals Rev.* **1997**, *41*, 66-75; b) D. Troegel, J. Stohrer, *Coord. Chem. Rev.* **2011**, *255*, 1440-1459; c) M. Pagliaro, R. Ciriminna, V. Pandarus, F. Beland, *Eur. J. Org. Chem.* **2013**, 6227-6235; d) D. A. Rooke, Z. A. Menard, E. M. Ferreira, *Tetrahedron* **2014**, *70*, 4232-4244; e) Y. Nakajima, S. Shimada, *RSC Adv.* **2015**, *5*, 20603-20616.
- [33] In some of the catalytic reactions collected in Table 1, the formation of minor amounts of a byproduct were detected by GC. According to ESI-HRMS measurements, this byproduct could be the disiloxane Me₂PhSiOSiPhMe₂ ([M]⁺ ion peak at *m/z* 287.1279), probably arising from the presence of adventitious water.
- [34] Although we have not carried out mechanistic studies, we assume that the catalytic reaction proceeds through a classical pathway in which the alcohol molecule attacks the silane once activated by coordination to the metal (see reference 29). In this regard, recent reports have confirmed the existence of cationic Pt(II) σ-silane complexes and their involvement in dehydrocoupling reactions of silanes and amines: a) P. Ríos, J. Díez, J. López-Serrano, A. Rodríguez, S. Conejero, *Chem. Eur. J.* **2016**, *22*, 16791-16795; b) P. Ríos, M. Roselló-Merino, O. Rivada-Wheelaghan, J.

-
- Borge, J. López-Serrano, S. Conejero, *Chem. Commun.* **2018**, 54, 619-622; c) P. Ríos, H. Fouilloux, P. Vidossich, J. Díez, A. Lledós, S. Conejero, *Angew. Chem.* **2018**, 130, 3271-3275; *Angew. Chem. Int. Ed.* **2018**, 57, 3217-3221.
- [35] This fact is in agreement with the decrease in the efficiency of complex **5** observed when carrying out the catalytic reaction in the presence of 500 equiv. of NaCl (42% conversion after 40 min; to be compared with entry 3).
- [36] W. L. F. Armarego, C. L. L. Chai, *Purification of Laboratory Chemicals*, 5th Ed., Butterworth-Heinemann, Oxford, **2003**.
- [37] D. R. Drew, J. R. Doyle, *Inorg. Synth.* **1990**, 28, 346.
- [38] E. Costa, P. G. Pringle, M. Ravetz, *Inorg. Synth.* **1997**, 31, 284-286.
- [39] L. D. Boardman, R. A. Newmark, *Magn. Reson. Chem.* **1992**, 30, 481-489.
- [40] a) C. A. Ghilardi, S. Midollini, S. Moneti, A. Orlandini, G. Scapacci, *J. Chem. Soc., Dalton Trans.* **1992**, 3371-3376; b) S. Antonaroli, B. Crociani, *J. Organomet. Chem.* **1998**, 560, 137-146.
- [41] *CrysAlis^{Pro}* 1.171.38.43, Rigaku Oxford Diffraction, Yarnton, UK, **2015**.
- [42] P. T. Beurskens, G. Beurskens, R. de Gelder, S. Garcia-Granda, R. O. Gould, J. M. M. Smits, *The DIRDIF2008 Program System*, Crystallography Laboratory, University of Nijmegen, The Netherlands, **2008**.
- [43] G. M. Sheldrick, *Acta Crystallogr., Sect. C: Struct. Chem.* **2015**, 71, 3-8.
- [44] K. Brandenburg, H. Putz, *DIAMOND*, Crystal Impact GbR, Bonn, Germany, **1999**.
-
